Acta Crystallographica Section B
Structural Science
ISSN 0108-7681

Charge-density analysis in polymorphs of urea–barbituric acid co-crystals

Marlena Gryl,* Anna Krawczuk-Pantula and Katarzyna Stadnicka

Faculty of Chemistry, Jagiellonian University, Ingardena 3, 30–060 Kraków, Poland

Correspondence e-mail: gryl@chemia.uj.edu.pl

Received 18 June 2010
Accepted 17 January 2011

High-resolution single-crystal X-ray diffraction measurements at 100 K were performed for the two polymorphs of urea–barbituric acid co-crystals: (I) $P2_1/c$ and (II) Cc. Experimental and theoretical charge density and its properties were analysed for (I) and (II) in order to confirm the previous observation that in the polymorphs studied the barbituric acid molecules adopt different mesomeric forms, leading to different hydrogen-bond systems. Koch and Popelier criteria were applied to distinguish between hydrogen bonds and van der Waals interactions in the structures presented.

1. Introduction

In the last few years the phenomenon of polymorphism in co-crystals has gathered much attention. The factors which influence the creation of specific hydrogen-bond patterns in polymorphic forms are of fundamental interest in crystal engineering (Gryl *et al.*, 2008; Bond, 2009). Understanding (and eventually controlling) the molecular recognition and self-assembling of molecular building blocks could facilitate the preparation of materials with specific desired properties.

Experimental charge density determination seems to be an attractive tool for studying polymorphism phenomena (Munshi & Guru Row, 2006; Overgaard & Hibbs, 2004; Whitten *et al.*, 2004; Gopalan *et al.*, 2000). The stability of various polymorphic modifications and the correlation between the structure and function of the crystalline material could be explained on the basis of experimental charge-density studies. Topological properties, such as the Laplacian or electrostatic potential, are used to describe non-covalent interactions and thus gain a deeper insight into the structure of polymorphic forms of co-crystals.

Recent studies on the polymorphism of a barbituric acid–urea addition compound (1:1) resulted in the discovery of three polymorphic modifications (Gryl *et al.*, 2008). Their crystal structures follow the symmetry of space groups $P2_1/c$ (I), Cc (II) and $P\bar{1}$ (III). The main conclusion of the paper was the hypothesis that the polymorphism phenomenon originates from the existence of resonance structures of the barbituric acid molecule. Relationships between possible mesomeric forms of barbituric acid were derived from the tautomeric forms predicted by Delchev (2004) and Senthilkumar & Kolandaivel (2002) and are shown in Scheme 1. From the crystal structure analysis of the three polymorphic modifications it was possible to recognize electron displacement in the barbituric acid molecules towards the following mesomeric forms: *E* in (I), *B* in (II) and *E* and *A* in (III).

© 2011 International Union of Crystallography
Printed in Singapore – all rights reserved

Table 1
Experimental single-crystal X-ray diffraction data for (I) and (II).

For all structures: $C_4H_4N_2O_3{\cdot}CH_4N_2O$, M_r = 188.15, Z = 4. Experiments were carried out at 100 K with Mo $K\alpha$ radiation using a KappaCCD diffractometer. Absorption was corrected for by multi-scan methods, *HKL DENZO* and *SCALEPACK* (Otwinowski & Minor, 1997). Refinement was with 0 restraints. H-atom parameters were constrained.

	(I)	(II)
Crystal data		
Crystal system, space group	Monoclinic, $P2_1/c$	Monoclinic, Cc
a, b, c (Å)	7.8123 (1), 6.9384 (1), 14.1179 (3)	16.0474 (5), 5.0280 (2), 10.3879 (3)
β (°)	96.727 (8)	110.093 (2)
V (Å^3)	759.99 (2)	787.15 (5)
μ (mm^{-1})	0.14	0.14
Crystal size (mm)	0.45 × 0.37 × 0.05	0.35 × 0.32 × 0.15
Data collection		
T_{min}, T_{max}	0.939, 0.993	0.953, 0.980
θ_{max} (°)	47.60	52.50
Resolution (Å^{-1})	1.04	1.12
Spherical refinement (*SHELXL*97)		
No. of reflections measured	43 513	17 534
No. of reflections unique	13 521	6342
No. of reflections with $F^2 > 2\sigma(F^2)$	10 830	5464
No. of parameters	136	119
$R[F^2 > 2\sigma(F^2)]$, $wR(F^2)$, S	0.0452, 0.1252, 1.037	0.0496, 0.1263, 1.074
ρ_{max}, ρ_{min}, r.m.s. (e Å^{-3})	0.66, −0.44, 0.08	0.49, −0.41, 0.07
Multipolar refinement (XDLSM)		
No. of data in refinement [$I > 2\sigma(I)$]	5793	3775
No. of refined parameters	276	274
$R[I > 2\sigma(I)]$, $wR(I)$, S	0.036, 0.029, 1.358	0.038, 0.027, 1.036
N_{ref}, N_v	20.99	13.78
Max shift/e.s.d. in last cycle	< 10^{-3}	< 10^{-3}
Weighting scheme	$w_1 = 1/[\sigma^2(F_o)]$	$w_1 = 1/[\sigma^2(F_o)]$
ρ_{max}, ρ_{min}, r.m.s. (e Å^{-3})	0.333, −0.314, 0.070	0.302, −0.279, 0.066

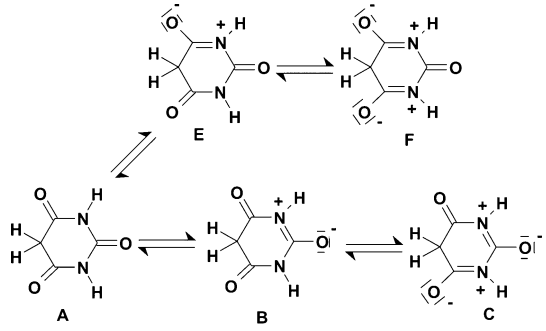

Scheme 1

In the present work we shall focus on two forms: $P2_1/c$ (I) and Cc (II). Comparative charge-density studies for polymorphs (I) and (II) were carried out to confirm the influence of the mesomeric effect on the mutual arrangement of barbituric acid and urea molecules.

2. Experimental

2.1. Sample preparation

Polymorphs of the barbituric acid and urea addition compound, with the chemical formula $C_4H_4N_2O_3{\cdot}CH_4N_2O$, were obtained under different crystallization conditions. Colourless crystals of (I) (space group $P2_1/c$) were obtained from a methanolic solution of barbituric acid and urea in the molar ratio 2:1. Crystals of (II), space group Cc, were obtained from an ethanolic solution of barbituric acid and urea in the molar ratio 1:2. The substrates were dissolved in the appropriate solvent at *ca* 323 K (in a water bath) and left to crystallize by slow evaporation at room temperature.

2.2. Spherical refinement

The structures of (I) and (II) were determined by single-crystal X-ray diffraction analysis at 100 K. Measurements were performed on a Nonius KappaCCD diffractometer (Nonius, 1997) equipped with an Oxford 700 Series Cryostream Cooler (Cosier & Glazer, 1986). For (I) three runs were recorded using ω scans at $\chi = 55°$ in order to collect accurate low- and high-angle data. For (II) two runs were recorded using ω scans at $\chi = 55°$. *HKL DENZO* and *SCALEPACK* (Otwinowski & Minor, 1997) were employed for cell refinement and data processing. Absorption corrections were introduced using a multi-scan procedure (Otwinowski & Minor, 1997). *SIR*92 (Altomare *et al.*, 1994) was used to solve the structures and structure refinement was carried out by *SHELXL*97 (Sheldrick, 2008). For (I) a total number of 43 513 reflections were sorted and merged by *SORTAV* (Blessing, 1997), assuming crystal class 2/*m*, giving 13 521 independent data. For (II) 17 534 reflections were collected over two runs and after sorting and merging procedures 6324 independent data were obtained assuming crystal class *m*. Space groups were assigned from the systematic absences observed in the diffraction patterns. In the case of polymorph (II) the $|E|$ distribution and $N(z)$ test clearly indicated a non-centrosymmetric space group. The structures were refined by full-matrix least-squares against F^2 using all data. The H atoms of amino and amido groups were found on difference-Fourier maps and refined in a riding model assuming $U_{iso} = 1.2U_{eq}$ of the parent atom. The H atoms of methylene groups were included in geometrically calculated positions and refined using a riding model with U_{iso}(H) = $1.2U_{eq}$(C5). Selected crystal data and experimental details are summarized in Table 1.

2.3. Multipole refinement

Multipole refinement was carried out using the Hansen–Coppens formalism (Hansen & Coppens, 1978) implemented in the *XD*2006 program package (Volkov *et al.*, 2006). The aspherical atom electron density is given by

$$\rho(r) = \rho_c(r) + P_v\kappa^3\rho_v(r) + \sum_{l=0}^{l}\kappa^3 R_l(\kappa' r)\sum_{m=0}^{l} P_{lm\pm}d_{lm\pm}(\theta,\varphi), \quad (1)$$

where ρ_c and ρ_v are the core and spherical valence densities, $d_{lm\pm}$ represents spherical harmonic angular functions, R_l is the radial function, κ and κ' are the expansion and contraction parameters, and P_v and $P_{lm\pm}$ represent the population parameters. The function minimized in the least-squares procedure was $\sum w(|F_o| - k|F_c|)^2$, with only those reflections included in the refinement which fulfil the criterion $I > 2\sigma(I)$. The multipole expansion was truncated at the octapole level for the C, N and O atoms and at the dipole level for H atoms. The κ and κ' parameters were employed for C, N and O atoms. The expansion and contraction parameters of the H atoms were fixed at the value of 1.13 for κ and 1.29 for κ' (Volkov *et al.*, 2001). High-order refinement ($\sin\theta/\lambda \geq 0.7$ Å^{-1}) for non-H atoms was performed in order to obtain accurate positional and displacement parameters. Low-order refinement ($\sin\theta/\lambda \leq 0.7$ Å^{-1}) was carried out to obtain accurate displacement parameters for the H atoms. The hydrogen positional parameters were fixed at the neutron determined distances of 1.092 Å for C—H and 1.009 Å for N—H (*International Tables for Crystallography*, 1995, Vol. C; Allen & Bruno, 2010). In the absence of neutron diffraction data, the H-atom anisotropic displacement parameters (a.d.p.'s) were estimated by using the *SHADE*2 web server (Madsen, 2006) and the obtained values were subsequently kept fixed during the refinement. The difference mean-square displacement amplitudes (DMSDA) for all bonds involving non H-atoms were within Hirshfeld limits (Hirshfeld, 1976). All static, residual, dynamic and deformation maps were analyzed using the *XDGRAPH* option plots. Iso-surface plots were obtained using the *MOLISO* program (Hübschle & Luger, 2006) and the exact experimental electrostatic potentials (Volkov *et al.*, 2004) were calculated using the EP/MM hybrid method as implemented in *XD*2006.

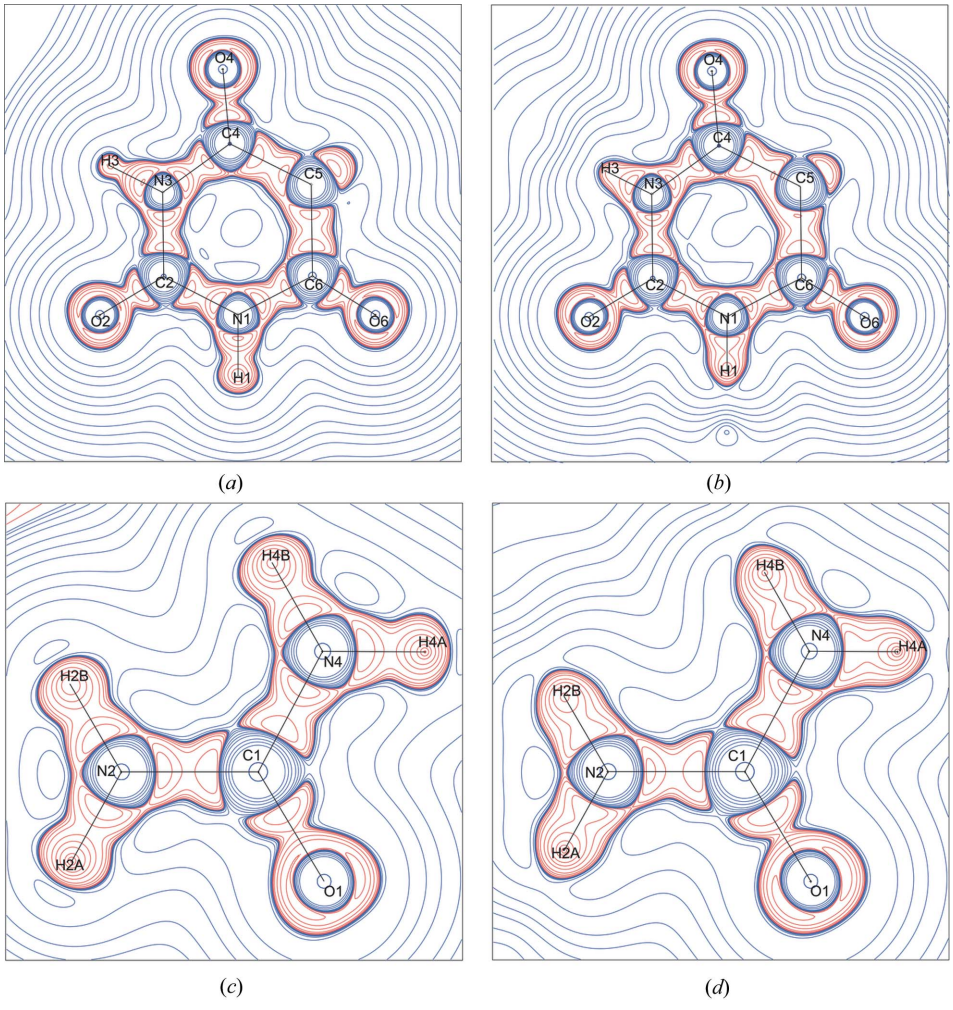

Figure 1
(*a*) and (*c*) Experimental, and (*b*) and (*d*) theoretical Laplacian maps of barbituric acid and urea molecules in polymorph (I). Contours are at logarithmic intervals in $-\nabla^2\rho(r)$ e Å^{-5}.

2.4. Theoretical calculations

Periodic single-point quantum calculations were performed using *CRYSTAL*06 (Dovesi *et al.*, 2006) with the DFT method at the B3LYP/6-31G** level of theory. The 6-31G** basis set was chosen deliberately because it has proven to give reasonable results for intermolecular interaction analysis (Munshi *et al.*, 2006). The geometry of the molecules was taken from the experimental results and was not optimized. The multipole refinement based on the amplitude of the theoretical static structure factors was carried out with the *XD*2006 program package. All the atomic positions were taken from the experiment and fixed during the refinement procedure, whereas the displacement parameters were set to zero and not refined. No restraints were imposed on the refined parameters. The multipoles and the kappa parameters were

Table 2
Experimental topological analysis of bond-critical points for (I) and (II).

$\rho(r)$ (e Å^{-3}) – charge density, Laplacian – $\nabla^2\rho(r)$ (e Å^{-5}) and eigenvalues of Hessian – λ_1, λ_2, λ_3 (e Å^{-5}), R_{ij} – internuclear separations (Å), d_1, d_2 – distance between BCP and atoms 1 and 2 (Å), ε – ellipticity. Top line: experimental values; second line (*italic*): theoretical values from periodic (*CRYSTAL*06) calculations.

Interaction	$\rho(r)$	$\nabla^2\rho(r)$	R_{ij}	d_1	d_2	λ_1	λ_2	λ_3	ε
(I)									
O2—C2	2.96 (4)	−37.40 (2)	1.224	0.766	0.458	−29.14	−25.90	17.64	0.13
	2.95 (8)	*−38.34 (4)*	*1.223*	*0.748*	*0.474*	*−27.76*	*−23.98*	*13.39*	*0.16*
O4—C4	2.92 (2)	−36.23 (1)	1.232	0.756	0.476	−27.92	−25.34	17.04	0.10
	2.91 (6)	*−37.63 (3)*	*1.231*	*0.760*	*0.471*	*−27.01*	*−23.78*	*13.16*	*0.14*
O6—C6	2.97 (1)	−37.02 (1)	1.219	0.758	0.461	−28.97	−26.38	18.34	0.10
	2.96 (1)	*−37.60 (1)*	*1.218*	*0.764*	*0.454*	*−28.07*	*−24.76*	*15.23*	*0.13*
O1—C1	2.70 (3)	−33.95 (2)	1.258	0.769	0.488	−25.79	−22.54	14.38	0.14
	2.73 (8)	*−31.76 (4)*	*1.260*	*0.742*	*0.518*	*−24.50*	*−21.33*	*14.07*	*0.15*
N1—C2	2.19 (2)	−22.52 (1)	1.371	0.818	0.552	−18.90	−15.80	12.17	0.20
	2.21 (7)	*−20.55 (2)*	*1.371*	*0.782*	*0.588*	*−19.02*	*−15.34*	*13.81*	*0.24*
N1—C6	2.15 (1)	−19.94 (1)	1.378	0.808	0.570	−18.38	−15.51	13.95	0.19
	2.16 (3)	*−19.14 (6)*	*1.379*	*0.785*	*0.593*	*−18.05*	*−14.87*	*13.77*	*0.21*
N1—H1	1.91 (2)	−24.64 (2)	1.009	0.791	0.218	−28.00	−26.74	30.09	0.05
	3.18 (1)	*−71.82 (1)*	*0.880*	*0.670*	*0.210*	*−54.13*	*−51.78*	*34.09*	*0.05*
N3—C2	2.19 (3)	−21.30 (1)	1.383	0.805	0.578	−19.17	−15.92	13.79	0.20
	2.06 (7)	*−15.23 (1)*	*1.384*	*0.778*	*0.606*	*−16.75*	*−13.71*	*15.24*	*0.22*
N3—C4	2.21 (2)	−22.04 (1)	1.364	0.812	0.552	−19.03	−16.09	13.08	0.18
	2.12 (5)	*−16.69 (2)*	*1.364*	*0.771*	*0.593*	*−17.13*	*−14.05*	*14.49*	*0.22*
N3—H3	1.91 (1)	−24.64 (1)	1.009	0.792	0.218	−28.00	−26.74	30.09	0.05
	3.18 (1)	*−71.80 (1)*	*0.880*	*0.670*	*0.211*	*−54.26*	*−51.62*	*34.08*	*0.05*
N2—C1	2.43 (2)	−24.86 (1)	1.348	0.769	0.580	−21.82	−17.98	14.93	0.21
	2.32 (7)	*−23.60 (1)*	*1.348*	*0.770*	*0.578*	*−20.44*	*−16.05*	*12.89*	*0.27*
N2—H2*A*	2.11 (2)	−25.50 (1)	1.009	0.758	0.251	−28.52	−26.93	29.92	0.06
	3.07 (1)	*−60.76 (1)*	*0.893*	*0.666*	*0.226*	*−49.01*	*−45.81*	*34.05*	*0.07*
N2—H2*B*	2.12 (1)	−26.17 (2)	1.009	0.760	0.250	−28.86	−27.38	30.06	0.05
	3.24 (5)	*−71.21 (1)*	*0.866*	*0.656*	*0.210*	*−54.83*	*−51.67*	*35.29*	*0.06*
N4—C1	2.36 (3)	−24.42 (1)	1.345	0.780	0.566	−21.07	−17.01	13.66	0.24
	2.34 (8)	*−24.11 (1)*	*1.344*	*0.768*	*0.576*	*−20.75*	*−16.23*	*12.87*	*0.28*
N4—H4*A*	2.12 (1)	−26.18 (1)	1.009	0.760	0.250	−28.86	−27.39	30.07	0.05
	3.22 (1)	*−69.83 (1)*	*0.870*	*0.658*	*0.212*	*−54.04*	*−50.94*	*35.15*	*0.06*
N4—H4*B*	2.11 (1)	−25.50 (1)	1.009	0.758	0.252	−28.50	−26.90	29.91	0.06
	3.05 (1)	*−59.77 (1)*	*0.896*	*0.668*	*0.228*	*−48.44*	*−45.25*	*33.92*	*0.07*
C4—C5	1.75 (2)	−12.76 (1)	1.495	0.775	0.720	−13.03	−11.01	11.28	0.18
	1.77 (6)	*−12.14 (2)*	*1.496*	*0.788*	*0.708*	*−12.58*	*−11.18*	*11.62*	*0.12*
C5—C6	1.74 (2)	−12.55 (1)	1.502	0.726	0.776	−13.05	−10.94	11.44	0.19
	1.74 (6)	*−11.61 (1)*	*1.503*	*0.708*	*0.795*	*−12.30*	*−10.90*	*11.59*	*0.13*
C5—H5*A*	1.51 (2)	−10.76 (1)	1.092	0.768	0.324	−14.85	−13.76	17.85	0.08
	2.30 (1)	*−30.54 (1)*	*0.990*	*0.627*	*0.363*	*−22.93*	*−22.22*	*14.61*	*0.03*
C5—H5*B*	1.59 (2)	−11.91 (1)	1.092	0.780	0.312	−16.04	−14.90	19.03	0.08
	2.31 (8)	*−30.80 (1)*	*0.990*	*0.630*	*0.360*	*−23.14*	*−22.55*	*14.89*	*0.03*
(II)									
O2—C2	2.86 (7)	−34.96 (3)	1.230	0.735	0.495	−26.24	−24.91	16.19	0.05
	2.84 (1)	*−29.98 (1)*	*1.228*	*0.433*	*0.795*	*−26.32*	*−22.93*	*19.27*	*0.15*
O4—C4	2.98 (5)	−37.71 (3)	1.225	0.777	0.448	−29.56	−26.05	17.91	0.13
	2.84 (1)	*−28.33 (4)*	*1.225*	*0.431*	*0.794*	*−25.63*	*−23.46*	*20.76*	*0.09*
O6—C6	2.99 (1)	−38.03 (1)	1.223	0.776	0.447	−29.94	−26.33	18.24	0.14
	2.86 (1)	*−28.73 (1)*	*1.222*	*0.430*	*0.793*	*−26.04*	*−23.81*	*21.11*	*0.09*
O1—C1	2.42 (8)	−27.23 (4)	1.265	0.807	0.458	−23.71	−19.48	15.95	0.22
	2.59 (1)	*−28.85 (1)*	*1.267*	*0.823*	*0.444*	*−22.73*	*−20.27*	*14.15*	*0.12*
N1—C2	2.15 (5)	−21.14 (2)	1.376	0.808	0.568	−17.49	−15.98	12.34	0.09
	2.18 (1)	*−19.44 (1)*	*1.375*	*0.777*	*0.598*	*−17.99*	*−14.90*	*13.45*	*0.21*
N1—C6	2.27 (3)	−22.76 (4)	1.373	0.788	0.585	−19.60	−16.61	13.46	0.18
	2.17 (1)	*−18.67 (1)*	*1.373*	*0.591*	*0.783*	*−17.45*	*−14.62*	*13.40*	*0.19*
N1—H1	2.12 (9)	−26.37 (6)	1.009	0.766	0.243	−28.55	−27.05	29.24	0.06
	3.27 (1)	*−74.00 (8)*	*0.880*	*0.650*	*0.230*	*−54.90*	*−53.40*	*34.30*	*0.03*
N3—C2	2.19 (6)	−20.84 (2)	1.377	0.799	0.578	−18.48	−15.87	13.51	0.16
	2.19 (1)	*−19.10 (1)*	*1.375*	*0.601*	*0.775*	*−18.03*	*−14.76*	*13.68*	*0.22*
N3—C4	2.27 (5)	−22.56 (2)	1.373	0.788	0.585	−19.51	−16.52	13.48	0.18
	2.16 (1)	*−18.58 (2)*	*1.373*	*0.784*	*0.590*	*−17.28*	*−14.55*	*13.25*	*0.19*
N3—H3	2.12 (1)	−26.37 (1)	1.009	0.766	0.243	−28.56	−27.05	29.24	0.06
	3.28 (1)	*−74.01 (1)*	*0.880*	*0.650*	*0.230*	*−54.91*	*−53.41*	*34.30*	*0.03*
N2—C1	2.47 (1)	−24.39 (2)	1.345	0.748	0.597	−22.18	−17.73	15.52	0.25
	2.32 (1)	*−24.52 (1)*	*1.343*	*0.571*	*0.773*	*−19.55*	*−15.47*	*10.50*	*0.26*
N2—H2*A*	2.07 (7)	−28.81 (4)	1.009	0.765	0.244	−27.93	−26.75	25.87	0.04
	3.21 (1)	*−65.54 (3)*	*0.880*	*0.641*	*0.239*	*−50.25*	*−47.21*	*31.92*	*0.06*
N2—H2*B*	2.08 (2)	−28.97 (1)	1.009	0.766	0.243	−28.05	−26.81	25.89	0.05

Table 2 (continued)

Interaction	$\rho(r)$	$\nabla^2\rho(r)$	R_{ij}	d_1	d_2	λ_1	λ_2	λ_3	ε
	3.23 (1)	*−66.73 (3)*	*0.880*	*0.644*	*0.236*	*−51.03*	*−47.87*	*32.18*	*0.07*
N4—C1	2.36 (6)	−23.08 (4)	1.347	0.763	0.584	−28.14	−16.23	14.09	0.29
	2.36 (1)	*−24.68 (3)*	*1.344*	*0.575*	*0.769*	*−19.62*	*−15.81*	*10.75*	*0.24*
N4—H4*A*	2.08 (1)	−28.97 (1)	1.009	0.766	0.243	−28.05	−26.81	25.89	0.05
	3.23 (1)	*−66.82 (1)*	*0.880*	*0.644*	*0.236*	*−51.07*	*−47.93*	*32.18*	*0.07*
N4—H4*B*	2.08 (1)	−29.25 (1)	1.009	0.766	0.243	−28.14	−26.96	25.85	0.04
	3.21 (1)	*−65.54 (1)*	*0.880*	*0.641*	*0.239*	*−50.26*	*−47.22*	*31.93*	*0.06*
C4—C5	1.73 (3)	−12.16 (1)	1.505	0.794	0.711	−12.81	−10.63	11.28	0.20
	1.71 (1)	*−10.91 (2)*	*1.505*	*0.799*	*0.706*	*−11.92*	*−10.46*	*11.48*	*0.14*
C5—C6	1.71 (4)	−11.83 (1)	1.502	0.704	0.798	−12.73	−10.37	11.26	0.23
	1.72 (1)	*−11.36 (1)*	*1.504*	*0.703*	*0.800*	*−11.98*	*−10.78*	*11.40*	*0.11*
C5—H5*A*	1.66 (6)	−14.11 (2)	1.094	0.711	0.383	−14.83	−13.75	14.47	0.08
	2.28 (1)	*−29.58 (2)*	*0.990*	*0.615*	*0.375*	*−22.50*	*−21.86*	*14.78*	*0.03*
C5—H5*B*	1.74 (3)	−14.72 (1)	1.092	0.729	0.363	−15.89	−14.95	16.12	0.06
	2.28 (1)	*−29.40 (1)*	*0.990*	*0.615*	*0.375*	*−22.38*	*−21.83*	*14.81*	*0.03*

refined according to the scheme used in the experimental data refinement. This was done in order to accurately compare the experimental and theoretical results obtained from multipole refinements. Topological analysis was carried out using *XDPROP* and atomic basin properties were calculated for all atoms using the *TOPINT* procedure included in *XD*2006. Additionally single-point calculations for isolated molecules of urea and barbituric acid were performed, using *GAUSSIAN*09 (Frisch *et al.*, 2009) at the B3LYP/6-31G** level of theory to evaluate the Koch & Popelier criteria. Quantum theory of atoms in molecules (QTAIM) analysis for isolated molecules of barbituric acid and urea was carried out using the *AIMA*II program (Keith, 2010).

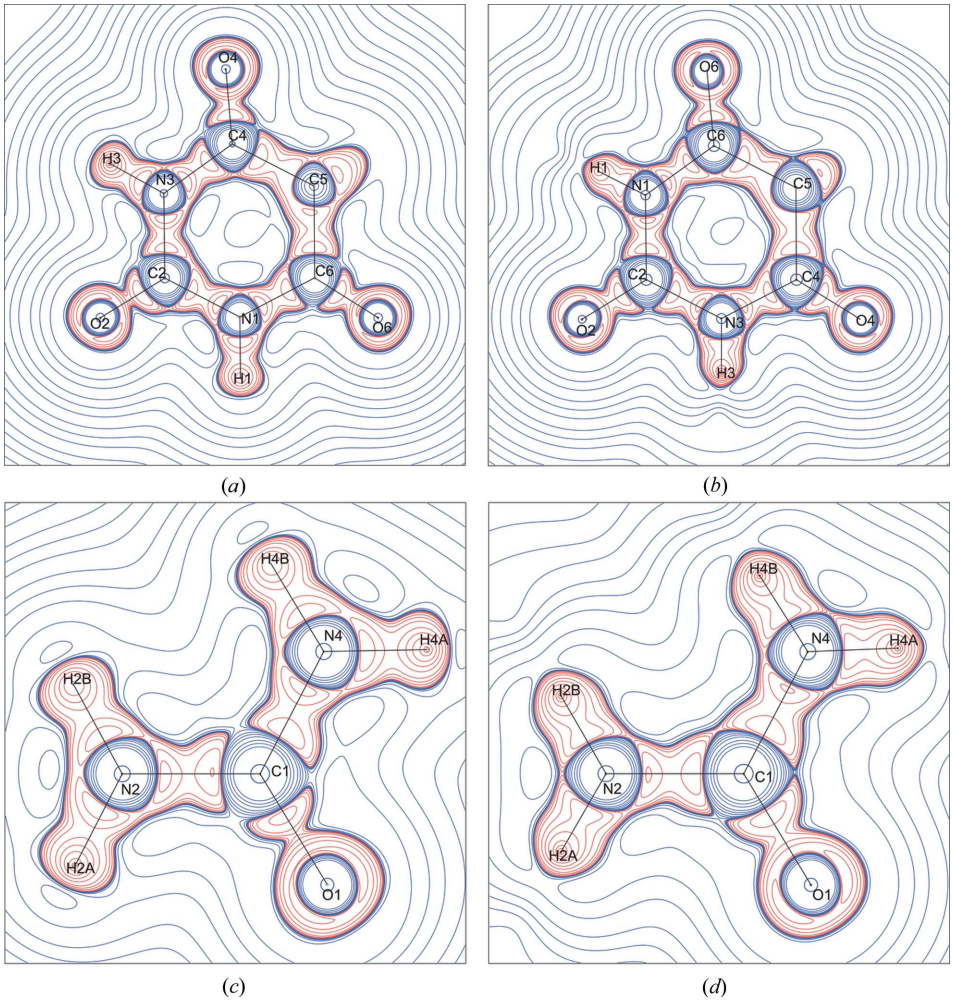

Figure 2
(*a*) and (*c*) experimental, and (*b*) and (*d*) theoretical Laplacian maps of barbituric acid and urea molecules in polymorph (II). Contours are at logarithmic intervals in $-\nabla^2\rho(r)$ e Å^{-5}.

3. Results and discussion

3.1. Structural details

The polymorphs examined differ in the mutual arrangement of barbituric acid and urea molecules, as has been previously shown (Gryl *et al.*, 2008). The asymmetric unit of (I), space group $P2_1/c$, is comprised of the barbituric acid and the urea molecules at the closest distance of C1 to the gravity centre of the ring (*ca* 3.24 Å) with the urea–1,3-diyl parts of the molecules situated parallel to each other. In (II), space group *Cc*, the barbituric acid and the urea molecules at the closest distance (*ca* 3.68 Å) are oriented anti-parallel to each other. Both structures are built of alternate layers of barbituric acid and urea mole-

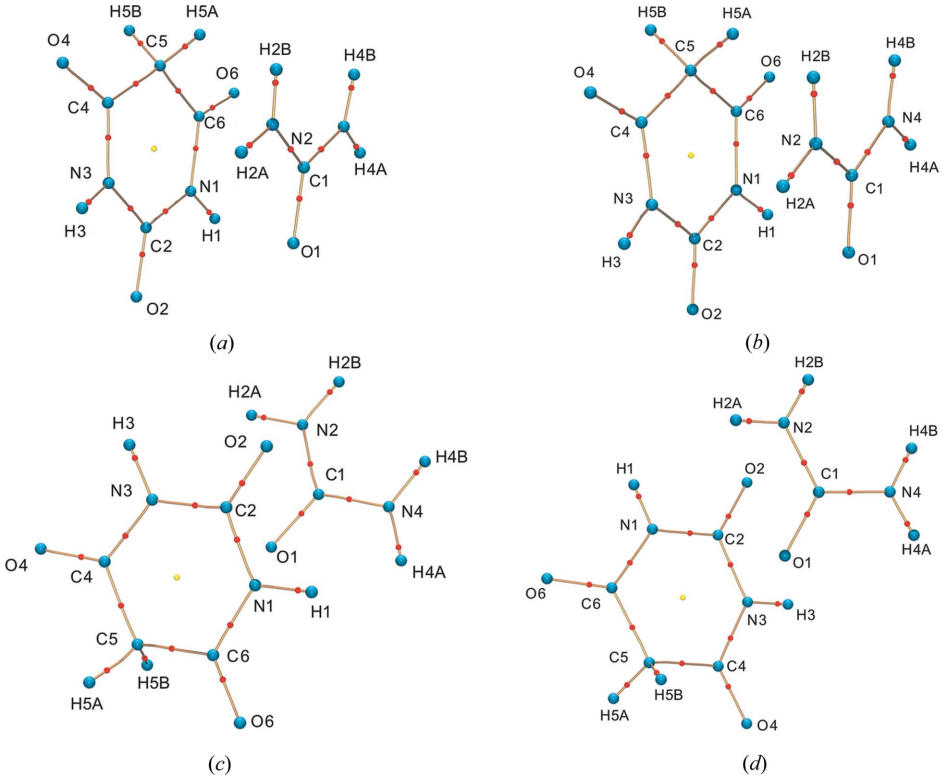

Figure 3
(*a*) and (*c*) experimental, and (*b*) and (*d*) theoretical molecular graphs for (I) (*a*), (*b*) and (II) (*c*), (*d*). Blue spheres indicate the atomic positions, red spheres the (3, −1) bond-critical points and yellow spheres the (3, +1) ring-critical points. The experimental charge density $\rho(r)$ values in the ring-critical point found for (I) and (II) are: 0.17 and 0.16 e Å^{-3}.

Table 3
Atomic net charges (q) for carbonyl O atoms and N atoms in (I) and (II).

q(Pv) – multipole net charges; q(s) – stockholder net charges; $q(\Omega)$ – charges derived from QTAIM.

	Experiment			Theory
Atom	q(Pv)	q(s)	$q(\Omega)$	$q(\Omega)$
(I)				
O2	−0.352	−0.365	−0.820	−0.891
O4	−0.295	−0.287	−0.828	−0.920
O6	−0.296	−0.284	−0.859	−0.951
O1	−0.296	−0.293	−0.884	−0.904
N1	−0.455	−0.118	−0.968	−0.906
N3	−0.455	−0.150	−0.972	−0.900
N2	−0.304	−0.163	−1.044	−0.934
N4	−0.305	−0.149	−1.039	−0.939
(II)				
O2	−0.041	−0.137	−0.774	−0.871
O4	−0.173	−0.262	−1.050	−0.951
O6	−0.173	−0.260	−1.072	−0.949
O1	−0.183	−0.157	−0.815	−1.062
N1	−0.214	−0.129	−1.317	−0.982
N3	−0.215	−0.131	−1.293	−0.980
N2	−0.294	−0.189	−1.416	−1.313
N4	−0.294	−0.172	−1.421	−1.323

cules, parallel to *ab* in (I) and to *bc* in (II). However, the urea layers in (I) contain centrosymmetric dimers formed by N2—H2···O1 hydrogen bonds, contrary to (II). Bond lengths and angles obtained from multipolar refinement for both structures are summarized in Table S1 of the supplementary material.[1] The observed differences in the values of C2—O2, C4—O4, C6—O6, C4—C5 and C5—C6 bond lengths can be correlated with one of the mesomeric forms of barbituric acid: *E* in (I) and *B* in (II) (*cf.* Scheme 1 and Table S1). Packing diagrams for both polymorphs were presented in our previous work (Gryl *et al.*, 2008).

3.2. Analysis of the electron-density distribution

The experimental and theoretical topological properties are listed in Table 2. The experimental Laplacian maps in the plane of barbituric acid and in the plane of urea molecules, given in Figs. 1(*a*) and (*c*), and 2(*a*) and (*c*), show the characteristic features of the static deformation-density maps. The expected strong maxima are visible in the middle of the covalent bonds. The main differences in the Laplacian of (I) and (II) are observed for the carbonyl O atoms of barbituric acid molecules, and additionally for N—H bonds. There were no significant differences for urea molecules in (I) and (II). A clear correlation between the value of the appropriate negative Laplacian and the bond lengths was observed, such that a shorter bond gives a higher value of $-\nabla^2\rho(r)$. A similar correlation could be observed for the charge density itself, which also increased with shortened bond lengths (see supplementary material, Figs. S1 and S2). The theoretical Laplacian maps (Figs. 1*b* and *d*, and 2*b* and *d*) are in good agreement with the experimental data. The observed minor differences might be associated with the anisotropic displacement parameters included in the experimental refinement.

In order to explain the influence of the mesomeric forms of barbituric acid on the formation of polymorphs (I) and (II), the net atomic charges of O and N atoms were calculated both from experimental and theoretical charge densities (Table 3). The values of multipole and stockholder charges (Hirshfeld, 1977) are in good agreement with each other as they are based on the same partitioning model. The QTAIM charges (Bader, 1994) are generally larger from those obtained by other

[1] Supplementary data for this paper are available from the IUCr electronic archives (Reference: GW5010). Services for accessing these data are described at the back of the journal.

Table 4
Topological analysis of intermolecular interactions in CP (3, −1).

$\rho(\mathbf{r})$ (e Å^{-3}) – charge density, Laplacian – $\nabla^2\rho(\mathbf{r})$ (e Å^{-5}) and eigenvalues of Hessian – λ_1, λ_2, λ_3 (e Å^{-5}). R_{ij} – internuclear separations (Å), d_1, d_2 – distance between BCPs and atom 1, 2 (Å), ε – ellipticity. $G(\mathbf{r}_{CP})$ (e Å^{-5}), $V(\mathbf{r}_{CP})$ (e Å^{-5}) – local kinetic and local potential energy density, and $E(\mathbf{r}_{CP})$ (e Å^{-5}) – local energy density of the electrons. Top line: experimental values, second line (*italic*): theoretical values from periodic (*CRYSTAL*06) calculations.

Interaction	$\rho(\mathbf{r})$	$\nabla^2\rho(\mathbf{r})$	R_{ij}	d_1	d_2	λ_1	λ_2	λ_3	ε	$G(\mathbf{r}_{CP})$	$V(\mathbf{r}_{CP})$	$E(\mathbf{r}_{CP})$
(I)												
H1···O1^{i}	0.20 (1)	3.27 (1)	1.819	0.649	1.171	−1.07	−1.03	5.37	0.05	0.74	−0.66	0.08
	0.19 (5)	*1.83 (9)*	*1.936*	*0.728*	*1.208*	*−1.15*	*−1.08*	*4.05*	*0.06*	*0.48*	*−0.50*	*−0.02*
H3···O4^{ii}	0.15 (1)	2.49 (1)	1.937	0.716	1.222	−0.72	−0.68	3.89	0.05	0.53	−0.45	0.09
	0.13 (1)	*1.41 (1)*	*2.059*	*0.791*	*1.268*	*−0.79*	*−0.70*	*2.90*	*0.13*	*0.34*	*−0.32*	*0.02*
H2*A*···O1^{iii}	0.14 (1)	3.21 (1)	1.889	0.666	1.224	−0.68	−0.66	4.55	0.04	0.64	−0.47	0.16
	0.15 (3)	*1.64 (5)*	*1.999*	*0.756*	*1.243*	*−0.91*	*−0.89*	*3.43*	*0.02*	*0.40*	*−0.39*	*0.01*
H2*B*···O4^{iv}	0.05 (1)	1.22 (1)	2.282	0.872	1.410	−0.22	−0.19	1.63	0.12	0.22	−0.14	0.08
	0.12 (1)	*1.22 (1)*	*2.119*	*0.825*	*1.293*	*−0.66*	*−0.65*	*2.52*	*0.02*	*0.14*	*−0.11*	*0.02*
H4*A*···O2^{i}	0.10 (1)	2.60 (2)	1.988	0.709	1.279	−0.49	−0.47	3.55	0.03	0.50	−0.35	0.15
	0.07 (1)	*0.64 (1)*	*2.385*	*0.979*	*1.406*	*−0.31*	*−0.29*	*1.24*	*0.07*	*0.29*	*−0.27*	*0.02*
H4*B*···O2^{v}	0.11 (1)	1.91 (1)	2.115	0.829	1.286	−0.47	−0.45	2.83	0.05	0.39	−0.30	0.09
	0.09 (1)	*1.47 (1)*	*2.173*	*0.850*	*1.324*	*−0.47*	*−0.32*	*2.26*	*0.46*	*0.29*	*−0.22*	*0.07*
Symmetry codes: (i) $-x, -y, -z+1$; (ii) $-x+1, y-\frac{1}{2}, -z+\frac{3}{2}$; (iii) $-x+1, -y, -z+1$; (iv) $-x+1, -y+\frac{1}{2}, -z+\frac{3}{2}$; (v) $x, y+1, z$												
(II)												
H1···O1^{i}	0.25 (1)	3.75 (1)	1.766	0.624	1.142	−1.37	−1.32	6.45	0.04	0.92	−0.90	0.02
	0.20 1)	*1.75 (3)*	*1.900*	*0.706*	*1.194*	*−1.23*	*−1.16*	*4.14*	*0.06*	*0.49*	*−0.54*	*−0.05*
H3···O1^{ii}	0.22 (1)	3.23 (1)	1.828	0.673	1.155	−1.12	−1.06	5.41	0.05	0.77	−0.73	0.04
	0.18 (1)	*1.69 (1)*	*1.952*	*0.738*	*1.214*	*−1.02*	*−0.97*	*3.68*	*0.05*	*0.44*	*−0.46*	*−0.02*
H2*B*···O4^{iii}	0.11 (1)	2.39 (1)	1.974	0.697	1.277	−0.46	−0.46	3.31	0.01	0.47	−0.35	0.12
	0.13 (5)	*1.10 (1)*	*2.104*	*0.823*	*1.281*	*−0.68*	*−0.67*	*2.45*	*0.02*	*0.28*	*−0.28*	*0.00*
H2*A*···O2^{iv}	0.11 (1)	2.11 (1)	2.003	0.735	1.269	−0.48	−0.43	3.01	0.12	0.42	−0.32	0.10
	0.13 (1)	*1.13 (1)*	*2.106*	*0.820*	*1.286*	*−0.70*	*−0.69*	*2.52*	*0.02*	*0.28*	*−0.28*	*0.00*
H4*A*···O2^{v}	0.10 (1)	2.20 (1)	1.997	0.717	1.280	−0.42	−0.41	3.03	0.02	0.43	−0.31	0.06
	0.12 (1)	*1.11 (1)*	*2.129*	*0.832*	*1.298*	*−0.65*	*−0.64*	*2.39*	*0.02*	*0.27*	*−0.26*	*0.01*
H4*B*···O6^{vi}	0.14 (1)	2.45 (1)	1.965	0.720	1.245	−0.65	−0.59	3.68	0.10	0.51	−0.41	0.10
	0.13 (1)	*1.38 (1)*	*2.080*	*0.807*	*1.273*	*−0.70*	*−0.64*	*2.72*	*0.08*	*0.33*	*−0.31*	*0.02*
Symmetry codes: (i) $x, y-1, z$; (ii) $x, -y+1, z+\frac{1}{2}$; (iii) $x, -y, z-\frac{1}{2}$; (iv) $x+\frac{1}{2}, y-\frac{1}{2}, z$; (v) $x, y+1, z$; (vi) $x+\frac{1}{2}, -y+\frac{1}{2}, z+\frac{1}{2}$												

methods. The differences between the charges on O atoms of the barbituric acid molecule for (I) and (II) are profound and each type of atomic charge provides valuable information about chemical bonding. In (I) the O2 atom has the lowest negative net charge, whereas in (II) the net charge on O2 has the highest negative value amongst the carbonyl O atoms of the barbituric acid molecule. The charges on O4 and O6 atoms in (II) are similar. The charges and the bond-length values (Table S1) clearly indicate the shift in electron density in (II) towards the mesomeric form *B*. In (I) the theoretical and experimental QTAIM charges show a higher negative value for O4 than for O6 which indicates the previously predicted form *E*. On the contrary, the multipole and stockholder charges have similar values for both O4 and O6 atoms, which might indicate form *F*. However, the N3—C4 bond length is shorter than N1—C6, which again indicates form *E*.

All the expected BCPs (bond-critical points) for covalent bonds were found (Fig. 3) as well as all the BCPs for weak interactions (hydrogen bonds, Table 4). In order to distinguish between the van der Waals interactions and hydrogen bonds, a special set of criteria had to be applied. The existence of the BCPs did not specify the type of bond formed, thus Koch & Popelier (1995) proposed eight criteria in order to determine the existence of hydrogen bonds. The first four criteria, concerning:

(i) the existence of the bond path between a donor and an acceptor atom,

(ii) the presence of non-zero charge density at the evaluated BCP and its relation with the overall hydrogen-bond energy,

(iii) a positive value of the Laplacian at the BCP and its correlation with the interaction energies, and

(iv) a mutual penetration of the H atom and the acceptor atom,

all could be obtained from the experimental charge-density analysis (Farrugia *et al.*, 2009). In order to evaluate the fourth criterion, described as 'necessary and sufficient' for characterization of a hydrogen bond (Munshi & Guru Row, 2005), the non-bonded radii of the hydrogen acceptor (taken as the gas phase van der Waals radii) were compared with the corresponding bonding radii (taken as the distance from the BCP to the nucleus). Both conditions for a positive interpenetration of van der Waals spheres of the donor and acceptor atoms were fulfilled: $\Delta r_H > \Delta r_A$ and $\Delta r_H + \Delta r_A > 0$ (Table 5). The local kinetic and potential energy densities were calculated from the charge densities for both polymorphs (Table 4). The relationships between $G(\mathbf{r}_{CP})$ and R_{ij} as well as $V(\mathbf{r}_{CP})$ and R_{ij} follow the exponential dependence, which can be seen in Fig. S3 of the supplementary material. At the BCPs, non-zero charge densities were evaluated and the Laplacians were found to have positive values.

Taking all this into consideration it is clear that all of the four Koch and Popelier criteria were fulfilled for polymorphs (I) and (II). The remaining four conditions, related to Bader's quantum theory of atoms in molecules, are difficult to estimate from experimental procedures. In order to evaluate those criteria the calculation of the net charges, atomic potential energies, atomic dipolar population and atomic volumes of H atoms involved in hydrogen bonding were performed for the crystal structures of both polymorphs and for isolated molecules of barbituric acid and urea. The results are summarized in Tables 6 and 7. The increasing net charge and potential energy values of H atoms going from isolated molecules to crystal structure can be observed for (I) and (II). As expected, the atomic polarization and atomic volume values decrease going from an isolated molecule to the crystal structure. A slight deviation from these criteria can be observed for both forms.

The results of the topological analysis of the hydrogen bonds, given in Table 4, revealed the distinct accepting properties of the carbonyl O atoms in the polymorphs, which is in agreement with our earlier suggestions. In (I), only the O6 atom is not an acceptor of a hydrogen bond, instead the O atom is a short distance from the centre Cg1 of the barbituric acid ring from the neighbouring layer [$C6^{i}—O6^{i}\cdots Cg1$: 1.2188 (5), 2.842 (1) Å; 129.9 (1)°; (i) $-x, y-\frac{1}{2}, -z+\frac{3}{2}$]. The area around the $Cg1\cdots O6^{i}$ interaction marked on the Hirshfeld surface, mapped with shape index, is shown in Fig. 6(*d*).

In (II) all the acceptor O atoms and all the donor N atoms are engaged in hydrogen-bond formation and, contrary to (I), there are no moderate hydrogen bonds between molecules of the same type (Table 4).

In the polymorphs described a lack of electron density at the centre of the barbituric heterocyclic ring was observed, in agreement with the results of the charge-density investigation for polymorph (II) of barbital at 198 K (Craven *et al.*, 1982). The RCPs (ring-criticial points) for the barbituric acid ring were found for the structures of (I) and (II), both from the experimental and theoretical approach (Fig. 3).

3.3. Electrostatic potential and Hirshfeld surfaces

Electrostatic potentials for urea and barbituric acid molecules were calculated from the experimental and theoretical charge density and visualized with the program *MOLISO* (Hübschle & Luger, 2006). In the two forms (I) and (II) the characteristic regions of positive potential, attracting the nucleophiles, and negative potentials, attracting electrophiles, are visible and well separated (Fig. 4). The observed differences in the nature of the potential on the O atoms between the two polymorphs are in agreement with our suggestion that the mesomeric forms influence the creation of specific hydrogen-bond patterns and thus lead to different polymorphic forms. From the viewpoint of the crystal nucleation in solution, the particular mesomeric form generated by the influence of urea and solvent molecules could produce a specific polymorph. In the case of form (I) ($P2_1/c$), comprised of urea dimers and the chains of barbituric acid molecules, there is a larger negative value of potential localized on the O2 atom than on O4 and O6 atoms. Contrary to (I), in (II) (*Cc*) a large negative potential

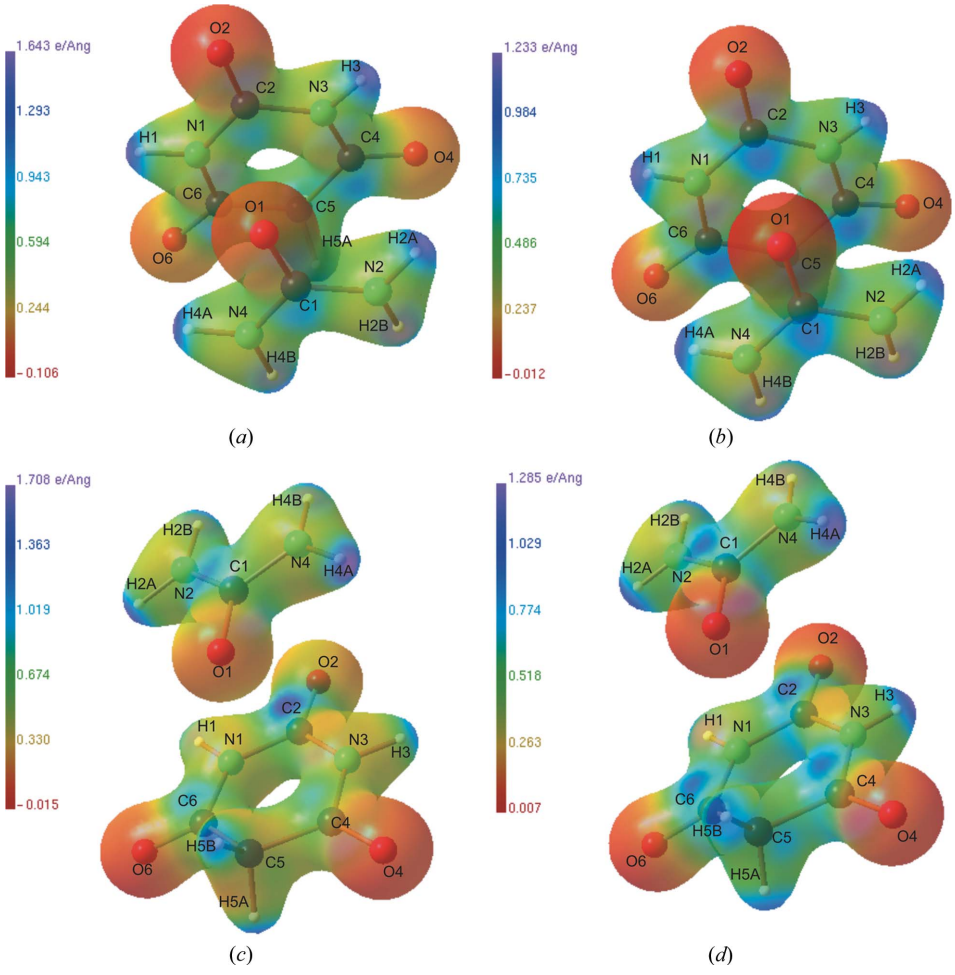

Figure 4
Three-dimensional representation of electrostatic potential calculated from (*a*) and (*c*) experimental, and (*b*) and (*d*) theoretical charge density. (*a*) and (*b*) for (I), (*c*) and (*d*) for (II), shown for the asymmetric units.

Table 5
Mutual penetration in terms of non-bonded radii (r_A^o, r_H^o) and bonded radii (r_A, r_H) of hydrogen and acceptor atoms.

$\Delta r_H = r_H^o - r_H$ and $\Delta r_A = r_A^o - r_A$. Top line: experimental values; second line (*italic*): theoretical values from periodic (*CRYSTAL*06) calculations.

Interaction	r_H	r_A	r_A^o	r_H^o	Δr_H	Δr_A	$\Delta r_H + \Delta r_A$
(I)							
H1···O1^{i}	0.649	1.171	1.420	1.060	0.411	0.250	0.661
	0.728	*1.208*	*1.420*	*1.060*	*0.332*	*0.213*	*0.544*
H3···O4^{ii}	0.716	1.222	1.420	1.060	0.344	0.198	0.543
	0.791	*1.268*	*1.420*	*1.060*	*0.269*	*0.152*	*0.421*
H2*A*···O1^{iii}	0.666	1.224	1.420	1.060	0.394	0.196	0.591
	0.756	*1.243*	*1.420*	*1.060*	*0.304*	*0.177*	*0.481*
H2*B*···O4^{iv}	0.872	1.410	1.420	1.060	0.188	0.010	0.198
	0.825	*1.293*	*1.420*	*1.060*	*0.235*	*0.127*	*0.362*
H4*A*···O2^{i}	0.709	1.279	1.420	1.060	0.351	0.141	0.492
	0.979	*1.406*	*1.420*	*1.060*	*0.081*	*0.014*	*0.095*
H4*B*···O2^{v}	0.829	1.286	1.420	1.060	0.231	0.134	0.365
	0.850	*1.324*	*1.420*	*1.060*	*0.210*	*0.096*	*0.307*
Symmetry codes: (i) $-x, -y, -z+1$; (ii) $-x+1, y-\frac{1}{2}, -z+\frac{3}{2}$; (iii) $-x+1, -y, -z+1$; (iv) $-x+1, -y+\frac{1}{2}, -z+\frac{3}{2}$; (v) $x, y+1, z$							
(II)							
H1···O1^{i}	0.624	1.142	1.420	1.060	0.436	0.278	0.714
	0.706	*1.194*	*1.420*	*1.060*	*0.354*	*0.226*	*0.580*
H3···O1^{ii}	0.673	1.155	1.420	1.060	0.387	0.265	0.652
	0.738	*1.214*	*1.420*	*1.060*	*0.322*	*0.206*	*0.528*
H2*B*···O4 ^{iii}	0.697	1.277	1.420	1.060	0.363	0.143	0.506
	0.823	*1.281*	*1.420*	*1.060*	*0.237*	*0.139*	*0.376*
H2*A*···O2^{iv}	0.735	1.269	1.420	1.060	0.325	0.151	0.476
	0.820	*1.286*	*1.420*	*1.060*	*0.241*	*0.134*	*0.374*
H4*A*···O2^{v}	0.717	1.280	1.420	1.060	0.343	0.140	0.483
	0.832	*1.298*	*1.420*	*1.060*	*0.228*	*0.123*	*0.351*
H4*B*···O6^{vi}	0.720	1.245	1.420	1.060	0.341	0.175	0.515
	0.807	*1.273*	*1.420*	*1.060*	*0.253*	*0.147*	*0.400*
Symmetry codes: (i) $x, y-1, z$; (ii) $x, -y+1, z+\frac{1}{2}$; (iii) $x, -y, z-\frac{1}{2}$; (iv) $x+\frac{1}{2}, y-\frac{1}{2}, z$; (v) $x, y+1, z$; (vi) $x+\frac{1}{2}, -y+\frac{1}{2}, z+\frac{1}{2}$							

Table 6
Atomic net charges (q), potential energy (E), atomic dipolar polarization (M) and atomic volume (V) for (I) and their corresponding differences (a.u.).

Index: ec – experimental values for crystal structure, tc – theoretical values for crystal structure and ti – theoretical values for the isolated molecules of urea and barbituric acid.

(I)	Crystal		DFT		
Atom	q_{ec}	q_{tc}	q_{ti}	$q_{ec} - q_{ti}$	$q_{tc} - q_{ti}$
H1	0.5742	0.5111	0.4650	0.1092	0.0461
H3	0.5742	0.5110	0.4650	0.1092	0.0461
H2*A*	0.5092	0.4426	0.4404	0.0688	0.0022
H2*B*	0.5104	0.4639	0.4404	0.0700	0.0235
H4*A*	0.5101	0.4604	0.4062	0.1039	0.0542
H4*B*	0.5090	0.4404	0.4062	0.1028	0.0342

(I)	Crystal		DFT		
Atom	E_{ec}	E_{tc}	E_{ti}	$E_{ec} - E_{ti}$	$E_{tc} - E_{ti}$
H1	−0.6805	−0.8598	−0.8400	0.1595	−0.0198
H3	−0.6805	−0.8598	−0.8400	0.1595	−0.0199
H2*A*	−0.8033	−0.9431	−0.9067	0.1033	−0.0364
H2*B*	−0.8027	−0.9253	−0.9066	0.1039	−0.0186
H4*A*	−0.8027	−0.9282	−0.8688	0.0661	−0.0594
H4*B*	−0.8037	−0.9451	−0.8688	0.0652	−0.0762

(I)	Crystal		DFT		
Atom	M_{ec}	M_{tc}	M_{ti}	$M_{ec} - M_{ti}$	$M_{tc} - M_{ti}$
H1	0.1489	0.1327	0.2126	−0.0638	−0.0799
H3	0.1487	0.1328	0.2126	−0.0640	−0.0799
H2*A*	0.1031	0.1362	0.2038	−0.1007	−0.0676
H2*B*	0.1038	0.1444	0.2038	−0.1000	−0.0594
H4*A*	0.1045	0.1443	0.1942	−0.0897	−0.0499
H4*B*	0.1028	0.1343	0.2038	−0.1010	−0.0695

(I)	Crystal		DFT		
Atom	V_{ec}	V_{tc}	V_{ti}	$V_{ec} - V_{ti}$	$V_{tc} - V_{ti}$
H1	22.14	16.84	61.19	−39.05	−44.35
H3	22.36	16.73	61.20	−38.84	−44.47
H2*A*	20.08	19.73	38.30	−18.22	−18.57
H2*B*	20.28	18.55	38.29	−18.01	−19.74
H4*A*	20.47	18.81	41.30	−20.82	−22.49
H4*B*	20.54	19.80	41.29	−20.75	−21.49

could be seen on the O4 and O6 atoms. In both polymorphs the O1 atoms of the urea molecules display a high negative potential. It is worth noting that O1 is situated in the close vicinity of the centre of the barbituric acid ring of a neighbouring molecule. The differences observed in the electrostatic potentials between the two forms can be related to the intermolecular interactions within the close environment of the appropriate barbituric acid or urea molecules. The theoretical results are in fairly good agreement with experiment. However, in theoretically calculated electrostatic potentials, the differences between the carbonyl O atoms are more obvious in (II).

Another way of differentiating between the polymorphs is through the visualization of the intermolecular interactions using Hirshfeld surfaces (Spackman & Jayatilaka, 2009). The Hirshfeld surfaces depend on the environment of a molecule in a crystal structure and are unique for a given polymorphic form. In (I) and (II) all the characteristic hydrogen bonds and other weak interactions, which were found earlier using topological analysis, were visualized by Hirshfeld surfaces mapped with d_{norm} (McKinnon *et al.*, 2007) and shown in Figs. 5 and 6. The contact areas shorter than the sum of the van der Waals radii were marked red; appropriate distances between hydrogen and acceptor atoms were also assigned. The light, almost transparent fragments of the surfaces represent the regions with low electron density. There are clear distinctions between the shapes of urea and barbituric acid Hirshfeld surfaces in both polymorphs. These reflect different packing of the molecules in those structures. In (I) the O6 atom lies in close proximity to the barbituric acid ring and the interaction is mapped with the shape index in Fig. 5(*d*). In (II) the urea O1 atom is approaching the barbiturate ring from one side, as can be seen in Fig. 6(*b*). The two interactions confirm the existence of negative charge deficiency in the centre of the barbituric acid ring. It is worth noting that in (II) there are no moderate hydrogen bonds between molecules of the same type.

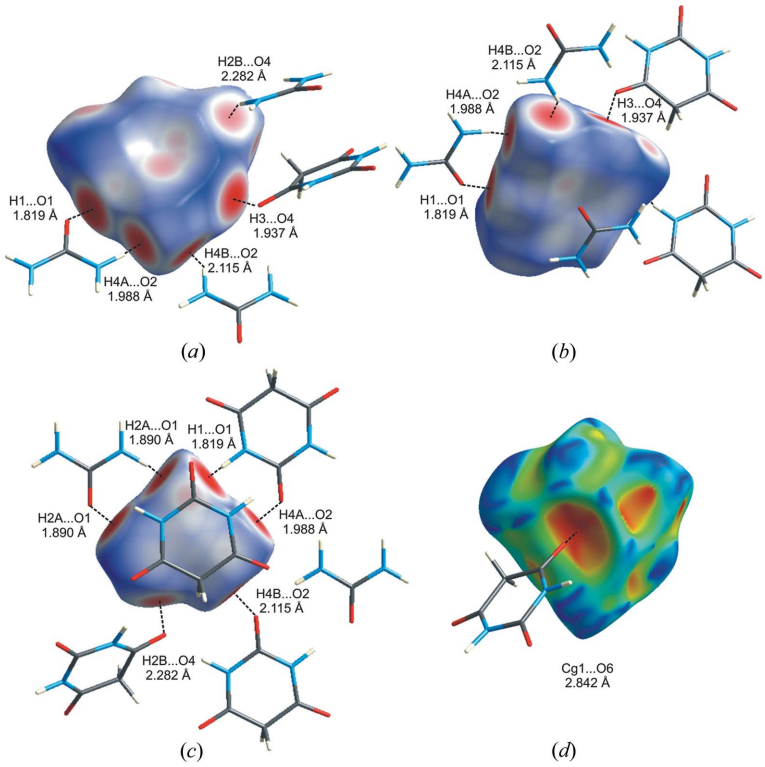

Figure 5
The Hirshfeld surfaces for (I): (*a*) and (*b*) barbituric acid molecule, (*c*) urea molecule, showing specific intermolecular contacts, (*d*) view of the Hirshfeld surface mapped with shape index in the area of the Cg1$\cdots$O6^{i} interaction.

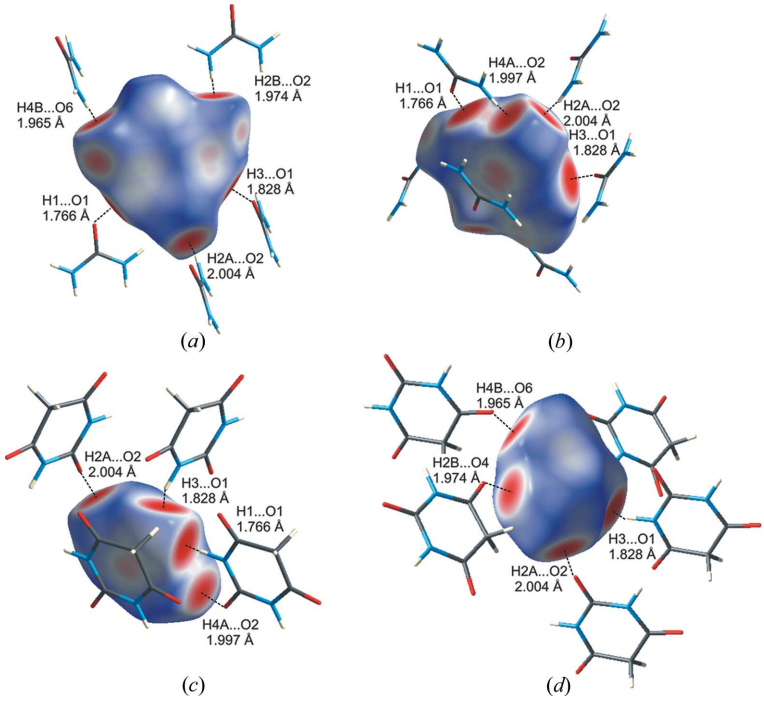

Figure 6
Hirshfeld surfaces for (II): (*a*) and (*b*) barbituric acid molecule, (*c*) and (*d*) urea molecule, highlighting intermolecular contacts. Hydrogen bonds are marked with dotted lines.

4. Conclusions

From experimental and theoretical charge-density studies, the geometries of the molecules of polymorphs (I) and (II) reported earlier (Gryl *et al.*, 2008) were confirmed and indicated the characteristic features of the mesomeric forms *E* and *B*. The BCPs were found for all covalent and hydrogen bonds. Moreover, the RCPs for the six-membered ring of the barbituric acid were defined. The electrostatic potential calculated for (II) had reflected a displacement of electron density towards the mesomeric form *B*. However, the electrostatic potential analysis did not show the expected significant differences between O4 and O6 behaviour in (I), as indicated for the mesomeric form *E*. The analysis of bond lengths and net charges calculated both from experimental and theoretical data clearly indicated the influence of the mesomeric forms of barbituric acid on the creation of polymorphs (I) and (II).

The displacement of electron density in the molecule of barbituric acid towards tautomeric forms of higher stability influences the type of hydrogen bond, which in turn determines various packing topology and different space groups in the polymorphs.

This work confirms a mutual relationship between the mesomeric form of the barbituric acid and the specific system of hydrogen bonds, which make the structures of the studied polymorphs (I) and (II) significantly distinct.

The authors thank the X-ray Diffraction Laboratory, Faculty of Chemistry, Jagiellonian University, for making the Nonius KappaCCD diffractometer available. This work was partially supported by the Polish Ministry of Science and Higher Education, Grant No. N N204 316537. The *GAUSSIAN*09 calculations were performed in the ACK 'Cyfronet' Computing Centre Kraków.

References

Allen, F. H. & Bruno, I. J. (2010). *Acta Cryst.* B**66**, 380–386.
Altomare, A., Cascarano, G., Giacovazzo, C., Guagliardi, A., Burla, M. C., Polidori, G. & Camalli, M. (1994). *J. Appl. Cryst.* **27**, 435–436.
Bader, R. (1994). *Atoms in Molecules. A Quantum Theory.* New York: Oxford University Press.
Blessing, R. H. (1997). *J. Appl. Cryst.* **30**, 421–426.
Bond, A. D. (2009). *Curr. Opin. Solid State Mater. Sci.* **13**, 91–97.
Cosier, J. & Glazer, A. M. (1986). *J. Appl. Cryst.* **19**, 105–107.
Craven, B. M., Fox, R. O. & Weber, H.-P. (1982). *Acta Cryst.* B**38**, 1942–1952.
Delchev, V. B. (2004). *J. Struct. Chem.* **45**, 570–578.

Table 7
Atomic net charges (q), potential energy (E), atomic dipolar polarization (M) and atomic volume (V) for (II), and their corresponding differences in a.u..

Index: ec – experimental values for crystal structure, tc – theoretical values for crystal structure and ti – theoretical values for the isolated molecules of urea and barbituric acid.

(II)	Crystal		DFT		
Atom	q_{ec}	q_{tc}	q_{ti}	$q_{ec} - q_{ti}$	$q_{tc} - q_{ti}$
H1	0.4398	0.5422	0.4650	−0.0252	0.0773
H3	0.4399	0.5476	0.4650	−0.0251	0.0826
H2*A*	0.5353	0.5345	0.4404	0.0948	0.0941
H2*B*	0.5420	0.5506	0.4404	0.1016	0.1102
H4*A*	0.5422	0.5517	0.4062	0.1360	0.1455
H4*B*	0.5358	0.5351	0.4062	0.1296	0.1289

(II)	Crystal		DFT		
Atom	E_{ec}	E_{tc}	E_{ti}	$E_{ec} - E_{ti}$	$E_{tc} - E_{ti}$
H1	−0.8224	−0.8510	−0.8400	0.0176	−0.0110
H3	−0.8223	−0.8472	−0.8400	0.0177	−0.0072
H2*A*	−0.7191	−0.8435	−0.9067	0.1876	0.0631
H2*B*	−0.7131	−0.8260	−0.9066	0.1936	0.0807
H4*A*	−0.7126	−0.8251	−0.8688	0.1563	0.0438
H4*B*	−0.7189	−0.8439	−0.8688	0.1499	0.0249

(II)	Crystal		DFT		
Atom	M_{ec}	M_{tc}	M_{ti}	$M_{ec} - M_{ti}$	$M_{tc} - M_{ti}$
H1	0.2246	0.1000	0.2126	0.0120	−0.1126
H3	0.2246	0.0953	0.2126	0.0120	−0.1173
H2*A*	0.1703	0.1038	0.2038	−0.0335	−0.1000
H2*B*	0.1708	0.1037	0.2038	−0.0330	−0.1001
H4*A*	0.1711	0.1025	0.1942	−0.0231	−0.0917
H4*B*	0.1710	0.1010	0.2038	−0.0328	−0.1028

(II)	Crystal		DFT		
Atom	V_{ec}	V_{tc}	V_{ti}	$V_{ec} - V_{ti}$	$V_{tc} - V_{ti}$
H1	31.24	12.51	61.19	−29.95	−48.68
H3	30.86	11.64	61.20	−30.34	−49.56
H2*A*	25.26	14.77	38.30	−13.04	−23.53
H2*B*	24.61	13.75	38.29	−13.68	−24.54
H4*A*	24.68	13.50	41.30	−16.62	−27.80
H4*B*	25.28	13.06	41.29	−16.01	−28.23

Dovesi, R., Saunders, V. R., Roetti, R., Orlando, R., Zicovich-Wilson, C. M., Pascale, F., Civalleri, B., Doll, K., Harrison, N. M., Bush, I. J., D'Arco, P. & Llunell, M. (2006). *CRYSTAL*06 *User's Manual.* University of Torino, Italy.

Farrugia, L. J., Kočovský, P., Senn, H. M. & Vyskočil, Š. (2009). *Acta Cryst.* B**65**, 757–769.

Frisch, M. J. *et al.* (2009). *GAUSSIAN*09, Revision A.1. Gaussian. Inc., Wallingford, CT, USA.

Gopalan, R. S., Kulkarni, G. U. & Rao, C. N. R. (2000). *ChemPhysChem*, **1**, 127–135.

Gryl, M., Krawczuk, A. & Stadnicka, K. (2008). *Acta Cryst.* B**64**, 623–632.

Hansen, N. K. & Coppens, P. (1978). *Acta Cryst.* A**34**, 909–921.

Hirshfeld, F. L. (1976). *Acta Cryst.* A**32**, 239–244.

Hirshfeld, F. L. (1977). *Theor. Chim. Acta*, **44**, 129–138.

Hübschle, C. B. & Luger, P. (2006). *J. Appl. Cryst.* **39**, 901–904.

Keith, T. A. (2010). *AIMA*II, Version 10.11.24, http://aim.tkgristmill.com.

Koch, U. & Popelier, P. L. A. (1995). *J. Phys. Chem.* **99**, 9747–9754.

Madsen, A. Ø. (2006). *J. Appl. Cryst.* **39**, 757–758.

McKinnon, J. J., Jayatilaka, D. & Spackman, M. A. (2007). *Chem. Commun.* pp. 3814–3816.

Munshi, P. & Guru Row, T. N. (2005). *Crystallogr. Rev.* **11**, 199–241.

Munshi, P. & Guru Row, T. N. (2006). *Cryst. Growth Des.* **6**, 708–717.

Munshi, P., Thakur, T. S., Guru Row, T. N. & Desiraju, G. R. (2006). *Acta Cryst.* B**62**, 118–127.

Nonius (1997). *COLLECT*. Nonius BV. Delft, The Netherlands.

Otwinowski, Z. & Minor, W. (1997). *Methods in Enzymology*, Vol. 276, *Macromolecular Crystallography*, part A, edited by C. W. Carter Jr & R. M. Sweet, p. 307. New York: Academic Press.

Overgaard, J. & Hibbs, D. E. (2004). *Acta Cryst.* A**60**, 480–487.

Senthilkumar, K. & Kolandaivel, P. (2002). *J. Comput. Aided Mol. Des.* **16**, 263–271.

Sheldrick, G. M. (2008). *Acta Cryst.* A**64**, 112–122.

Spackman, M. A. & Jayatilaka, D. (2009). *CrystEngComm*, **11**, 19–32.

Volkov, A., Abramov, Y. A. & Coppens, P. (2001). *Acta Cryst.* A**57**, 272–282.

Volkov, A., Koritsanszky, T. & Coppens, P. (2004). *Chem. Phys. Lett.* **391**, 170–175.

Volkov, T., Macchi, P., Farrugia, L. J., Gatti, C., Mallinson, P., Richter, T. & Koritsanszky, T. (2006). *XD*2006. University at Buffalo, State University of New York, NY, USA; University of Milano, Italy; University of Glasgow, UK; CNRISTM, Milano, Italy; Middle Tennessee State University, TN, USA.

Whitten, A. E., Dittrich, B., Spackman, M. A., Turner, P. & Brown, T. C. (2004). *Dalton Trans.* pp. 23–29.